

Mineralogy, geochemistry and Nd isotope composition of the Rainbow hydrothermal field, Mid-Atlantic Ridge

ANA FILIPA A. MARQUES¹ (✉)

FERNANDO J.A.S. BARRIGA¹

VALERIE CHAVAGNAC²

YVES FOUQUET³

¹Address: CREMINER / Dept. Geologia, Faculdade de Ciências, Universidade de Lisboa, Edifício C6, Piso 4, Campo Grande, 1749-016 Lisboa, Portugal

E mail: afamarques@fc.ul.pt
Telephone: 351 21 750 00 00 (ext. 26466)
Fax: 351 21 750 00 64

²Address: National Oceanography Centre, Southampton, European Way, Southampton SO14 3ZH, United Kingdom

³Address IFREMER, Centre de Brest, Plouzané BP 70, 29280 Plouzané, France

Abstract

Petrological, geochemical and Nd-isotopic analyses have been carried out on rock samples from the Rainbow vent field to assess the evolution of the hydrothermal system. The Rainbow vent field is an ultramafic-hosted hydrothermal system located on the Mid-Atlantic Ridge, characterized by vigorous high-temperature venting (~365°C) and unique chemical composition of fluids: high chlorinity, low pH and very high Fe and REE contents (Douville et al. 2002). Serpentinisation has occurred under a low-temperature (<270°C) retrograde regime, later overprinted by a higher temperature sulphide mineralisation event. Retrograde serpentinisation reactions alone cannot reproduce the reported heat and specific chemical features of Rainbow hydrothermal fluids. The following units were identified within the deposit: (1) non-mineralised serpentinite, (2) mineralised serpentinite – stockwork, (3) steatite, (4) semi-massive sulphides, and (5) massive sulphides which include Cu-rich massive sulphides (up to 28 wt% Cu) and Zn-rich massive sulphide chimneys (up to 5 wt% Zn). Sulphide mineralisation has produced significant changes in the sulphide-bearing rocks including enrichment in transition metals (Cu, Zn, Fe and Co) and LREE, increase in the Co/Ni ratios comparable to those of mafic Cu-rich VMS deposits and different $^{143}\text{Nd}/^{144}\text{Nd}$ isotope ratios. Vent fluid chemistry data are indicative of acidic, reducing and high temperature conditions at the seafloor reaction zone where fluids undergo phase separation most likely under sub-critical conditions (boiling). An explanation for the high chlorinity is not straightforward unless mixing with a high salinity brine or direct contribution from a magmatic Cl-rich aqueous fluid is considered. This study adds new data, which, combined with the current knowledge of the Rainbow vent field, brings compelling evidence for the presence, at depth, of a magmatic body, most likely gabbroic, which provides heat and metals to the system. Co/Ni ratios proved to be a good tool to discriminate between rock units, degree of sulphide mineralisation and positioning within the hydrothermal system. Deeper units have $\text{Co/Ni} < 1$ and subsurface and surface units have $\text{Co/Ni} > 1$.

Keywords: Massive sulphides, Serpentinite, Nd isotopes, Mid-Atlantic Ridge, Rainbow vent field.

Introduction

More than one hundred hydrothermal sites have been discovered over the past twenty-five years along the worldwide network of mid-ocean ridges (Baker and German 2004). Most hydrothermal sites are basalt-hosted, with seafloor venting corresponding to the visible part of a complex and vigorous fluid circulation system active at the sub-surface. A typical modern seafloor sulphide deposit encompasses a consolidated sulphide mound, underlain by a sub-seafloor stockwork and covered by active and inactive chimney structures, hydrothermal crusts, metalliferous sediments and sulphide debris (Goodfellow and Franklin 1993; Fouquet et al. 1993a, 1993b; Rona et al. 1993; Alt 1995; Hannington et al. 1995; Herzig and Hannington 1995; Humphries et al. 1995; Fouquet et al. 1996). These features, commonly found in modern seafloor deposits, correlate well with those of ancient volcanic-hosted massive sulphide (VMS) deposits (Doyle 2003). Both ancient ore-grade VMS deposits and their modern analogs result from sub-seafloor heat driven seawater circulation, reacting with crustal or upper mantle rocks, and producing syngenetic accumulations of massive sulphides hosted by submarine volcanic successions (Large 1992 and references therein; Barrie and Hannington 1997).

There is a strong relation between the base metal contents in VMS deposits and the nature of their host rocks (Barrie and Hannington 1997). Accordingly, VMS deposits (ancient and modern) can be divided into five categories: (1) mafic, (2) bimodal-mafic, (3) mafic-siliciclastic, (4) bimodal-felsic and (5) bimodal-siliciclastic. Mafic VMS are smaller, Cu-rich and Pb-poor deposits and are generally associated with synvolcanic intrusions considered to be the heat and metal sources (Barrie and Hannington 1997). Several modern seafloor sulphide deposits along the Mid-Atlantic Ridge (MAR) (e.g. TAG, MESO, Snake Pit) have characteristics comparable to those of mafic VMS deposits in which sediment-starved, high temperature deposits are Cu and Co rich with high Cu/Zn ratios, contrasting with lower

temperature sedimented ridges that are Zn and Pb-rich (Kase et al. 1990; German et al. 1993; Fouquet et al. 1993; Goodfellow and Franklin 1993; Rona et al. 1993; Tivey et al. 1995; Langmuir et al. 1997; Herzig et al. 1998; Münch et al. 1999; Charlou et al. 2000; Lawrie and Miller 2000; Douville et al. 2002). Although in mafic rocks Ni is in excess relative to Co, the related VMS host Co-rich sulphides, most likely due to the more chalcophile behaviour of Co (Hawley and Nichol 1961).

The recent discovery of ultramafic-hosted seafloor hydrothermal systems at the MAR adds a new perspective to the dynamics of seafloor hydrothermal processes and the influence of host rocks. So far, there are five known ultramafic-hosted hydrothermal sites at the MAR: Rainbow, Logatchev, Lost City, Saldanha and Menez Hom, all linked to serpentinisation reactions and high methane anomalies (Batuyev et al. 1994; German et al. 1996; Donval et al. 1997; Fouquet et al. 1998; Fouquet et al. 2001; Kelley 2001; Barriga et al. 2002). Rainbow and Logatchev are vigorous high-temperature systems with high bulk Cu/Zn ratios, high Cu and Co and low Pb, producing metal-rich black smoker fluids while Saldanha and Menez Hom are low temperature diffuse systems (<10°C) (Batuyev et al. 1994; Bogdanov et al. 1995; Lein et al. 2001; Fouquet et al. 2001; Douville et al. 2002; Barriga et al. 2002; Marques 2005 PhD thesis in preparation). The Lost City field contains carbonate-brucite chimneys venting high pH fluids (pH 9-10) at intermediate temperatures (40-75°C) (Kelley et al. 2001; Früh-Green et al. 2003; Allen and Seyfried 2004). Serpentinisation driven hydrothermalism seems to be the leading process occurring at Lost City, Saldanha and Menez Hom (Barriga et al. 1998, 2004; Kelley et al. 2001; Früh-Green et al. 2003; Allen and Seyfried 2004, Costa 2005).

The Rainbow hydrothermal vent field is a vigorous hydrothermal system hosted in completely serpentinised peridotites. Rainbow vent fluids are characterized by the highest temperature reported for MAR fluids (365°C), the highest chloride concentration (750 mM), the lowest end-member pH (2.8), high trace metal contents (Fe, Cu, Zn, Co, Ni) and high

REE and K, Rb and Cs contents (Douville et al. 2002). These unique physical and chemical characteristics have raised numerous questions concerning the processes acting at Rainbow. Recent cruises at the Rainbow hydrothermal vent field (e.g., HEAT cruise 1994; FLORES cruise 1997; IRIS cruise 2001) have enabled a thorough understanding of the tectonic setting, hydrothermal fluid and particle chemistry and the record of hydrothermal activity by sediment coring (German et al. 1996; Barriga et al. 1997; Donval et al. 1997; Douville et al. 1997; Parson et al. 1997; Gràcia et al. 2000; Cave et al. 2002; Douville et al. 2002; Edmonds and German 2004; Chavagnac et al. 2005). However, our knowledge of the sub-surface structure of the Rainbow active hydrothermal system remains very limited. Fluid interaction and mineralisation processes need to be addressed in order to reach a better understanding of the functioning of this ultramafic-hosted hydrothermal system.

In this paper, we present a detailed, comprehensive and thorough description of the geological setting, structure and mineralogy of the Rainbow hydrothermal sulphide deposit and underlying stockwork, from the rock precursor serpentinite to massive sulphides. The field data and sampling result not only from the cruises mentioned before but also, and mainly, from the SALDANHA (1998), IRIS (2001) and SEAHMA (2002) cruises (IRIS cruise report 2001; SALDANHA cruise report 1999; SEAHMA cruise report 2003). We have carried out geochemical and Nd isotope analyses to characterize the Rainbow hydrothermal deposit and to assess the evolution of its formation.

Geological Setting

The Rainbow hydrothermal vent field is located on the MAR at the inside corner of a non-transform offset, which links the second-order ridge segments AMAR and South AMAR (36°14'N; 33°53'W) (Fig. 1). The vent area is composed of a group of at least 10 black smokers expelling high-temperature (~365°C) fluids with evidence of phase separation at depth (Fouquet et al. 1997; Douville et al. 2002).

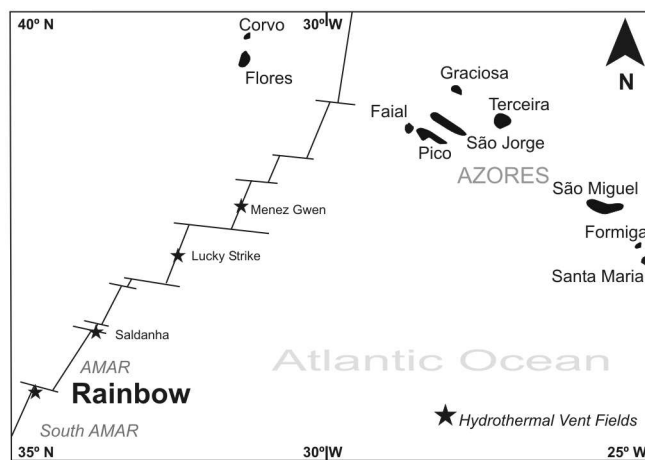


Fig. 1 Location of the Rainbow vent field in a non-transform offset between the AMAR and South AMAR second-order segments at the Mid-Atlantic Ridge (MAR), south of the Azores Islands

Field observations during ROV dives, IRIS and SEAHMA cruises, coupled with sample location data collected during the SEAHMA, IRIS and FLORES cruises have enabled the drafting of a detailed geological map of the vent field area (Fig. 2a) (FLORES cruise report 1998; SEAHMA cruise report 2002; IRIS cruise report 2001). In the Rainbow ridge area, completely serpentinised peridotite outcrops, covered by whitish pelagic sediment, are often crosscut by normal faults exposing the serpentinite. On the western limit of the active vent area, a sub-vertical normal fault trending N-S reveals ultramafic rocks with visible networks of sulphide-bearing veinlets (i.e. a well-defined stockwork). In the upper part of the scarp, sulphides become more abundant, occurring as semi-massive sulphides. The active

venting area contains numerous active and inactive sulphide chimneys that lie on top of sulphide mounds built up mostly by the accumulation of collapsed, dead chimneys. Basalt outcrops were found exclusively on the bottom of the South AMAR segment (W of Rainbow ridge) and at the easternmost section of the vent field area at the summit of the Rainbow ridge. The basalts at the ridge summit are pillow lavas and overlie the serpentinites. So far, no contact has been recognized (Fouquet et al. 1998). Figure 2b shows a geological profile which combines bathymetry with sample type and location (SEAHMA cruise) and ROV observations (SEAHMA cruise).

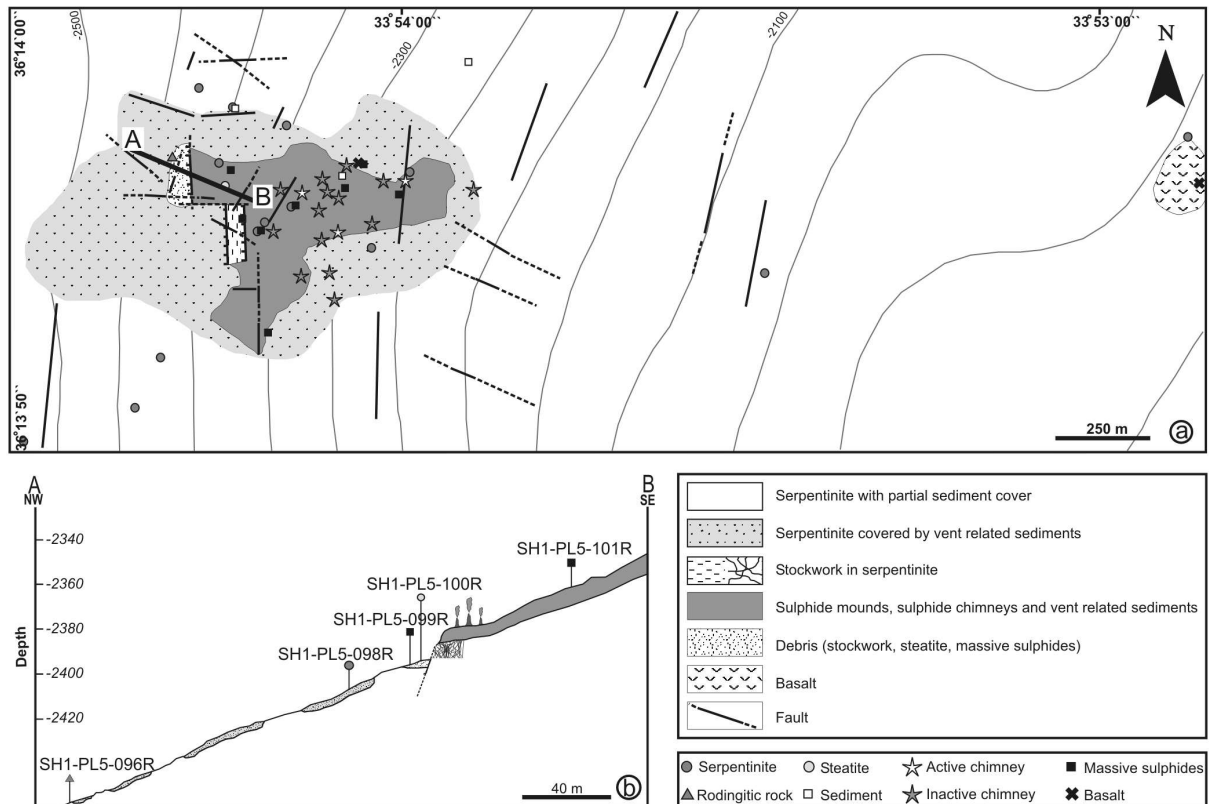


Fig. 2 a Geological map of the Rainbow vent field area with sample location (geology and sample location from direct observations during IRIS and SEAHMA 1 cruises and FLORES cruise report; bathymetric data and ADELIE software from IFREMER). Line AB is the cross-section represented in (b). **b** Interpretative geological cross-section, with no vertical exaggeration, representing location of samples collected during dive SH1-PL5 of the SEAHMA1 cruise

Sample Description

From the rock suite collected during the IRIS and SEAHMA cruises using ROV and dredges, 128 samples were selected. Of these, 71 have been carefully studied under transmitted and reflected light microscopy. Fig. 3 illustrates a paragenetic sequence in the Rainbow rocks and ores and Fig. 4 contains thin section microphotographs taken from representative samples of the ore deposit.

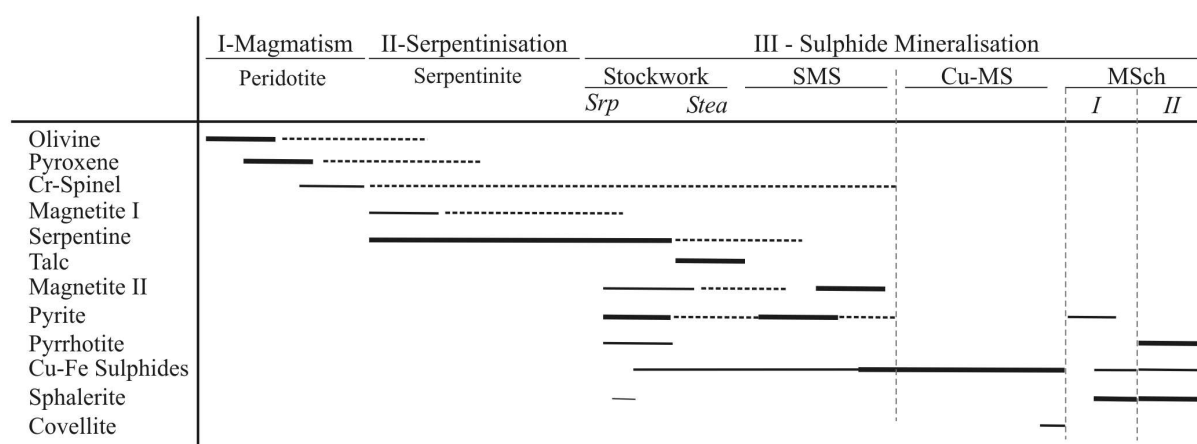


Fig. 3 Paragenetic sequence of minerals present in studied rocks from the Rainbow vent field. Increasing mineral abundances are represented by increasing line thickness. Abbreviations: *Srp* serpentinite, *Stea* steatite, *SMS* semi-massive sulphides, *Cu-MS* Cu massive sulphides, *MS ch* massive sulphide chimneys

Host rocks

Serpentinites (*Srp*) that form the substratum of the Rainbow vent field are non-deformed and comprise serpentine-group minerals (mainly lizardite) with well-preserved pseudomorphic textures (mesh, hourglass and bastite) dust-like euhedral grains of magnetite (mgt I) and accessory anhedral Cr-spinel with hydrothermally altered rims (Fig. 4a, b). These features correspond to serpentinites that resulted from simple peridotite-seawater interactions under static, low-temperature, retrograde metamorphism. Subsequent, sigmoidal cross-

fractures filled with fibrous γ -serpentine and carbonate-filled veins define the late and brittle deformation stage.

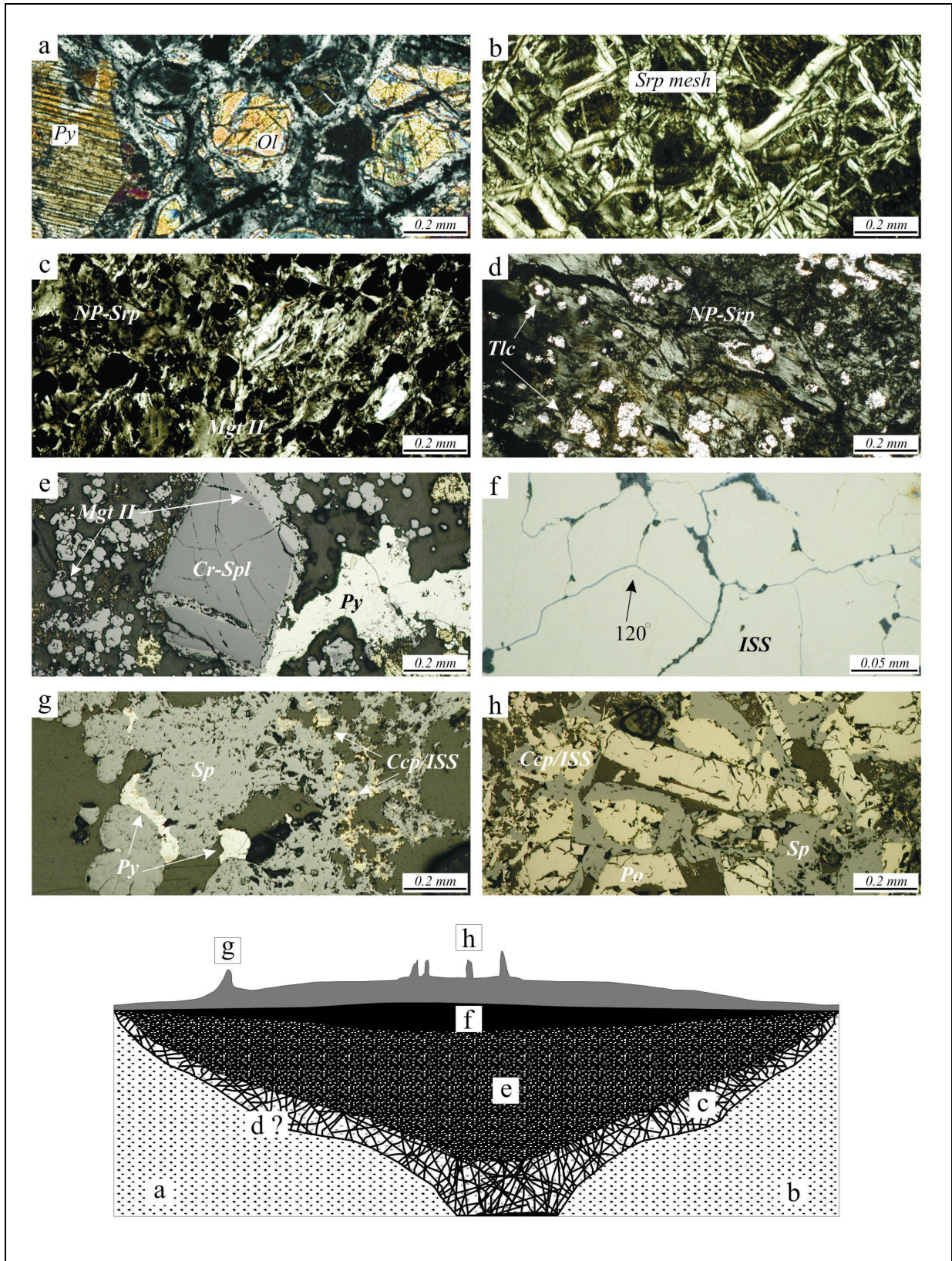


Fig. 4 Interpretative scheme through the active area of Rainbow vent field. Microphotographs taken under reflected light, except (a) (b), (c) and (d) taken with transmitted light with crossed nicols. **a** Partially serpentinised peridotite with pyroxene, olivine and serpentine mesh (after olivine). **b** Serpentinite with well-developed serpentine mesh texture after olivine. **c** Mineralised serpentinite (stockwork) with non-pseudomorphic featureless serpentine and coarse-grained magnetite II. **d** Transitional stage between stockwork and steatite where the non-pseudomorphic serpentine is gradually replaced by talc. **e** Semi-massive sulphide unit (SMS) with relics from the rock precursor (Cr-spinel and highly altered phyllosilicates). **f** Recrystallized Cu-rich massive sulphide unit (Cu-MS) with intermediate solid solution/chalcopyrite exhibiting 120° jointing. **g** Massive sulphide chimney (*type I*) with low temperature sulphide assemblage pyrite + Zn-sphalerite + chalcopyrite/intermediate solid solution. **h** Massive sulphide chimney (*type II*) with high temperature sulphide assemblage, pyrrhotite + Fe-sphalerite + intermediate solid solution/chalcopyrite. Abbreviations: *Ccp/ISS* exsolved chalcopyrite in intermediate solid solution, *Cr-spl* Cr-spinel, *ISS* intermediate solid solution, *Mgt II* magnetite II, *NP-srp* non-pseudomorphic serpentine, *Ol* olivine, *Po* pyrrhotite, *Px* pyroxene, *Py* pyrite, *Sp* sphalerite, *Srp mesh* serpentine with mesh texture, *Tlc* talc

Sulphide-bearing Zones

Progressive percolation of high-temperature mineralising hydrothermal fluids through the serpentinite induced the pervasive replacement of silicate mineralogical assemblages resulting in textural changes (Fig. 4c-h). The various sulphide-bearing rocks are described below.

Stockwork in serpentinite (St)

Pseudomorphic serpentine-group minerals, characteristic of serpentinites, are replaced by non-pseudomorphic featureless serpentine, mainly chrysotile (Fig. 4c). The earliest hydrothermal sulphides occur here, either disseminated or in veinlets and surrounded by the non-pseudomorphic serpentine matrix. Euhedral to anhedral pyrite (py) grains are ubiquitous and predate all other sulphide phases. Intermediate solid solution sulphides with exsolved

chalcopyrite (ISS/Ccp) occur mostly as spherical aggregates or small anhedral grains dispersed within the serpentine matrix and, occasionally, replace pyrite. Rarely, fine-grained covellite occurs as rims surrounding ISS/Ccp. Euhedral lamellar crystals of pyrrhotite (po) and less frequently sphalerite (sp) may occur. Dust-like magnetite (mgt I) produced during serpentinisation disappears and a new, coarse-grained magnetite (mgt II), indicative of late oxidizing conditions, occurs as individual and dispersed grains that often replace pyrite. Hydrothermally altered Cr-spinel relics (Cr-spl) reveal highly reflective borders of “ferritchromit”. Large, euhedral and radial prisms of aragonite occur along veins previously filled by sulphides.

Steatite (Stea)

Locally, stockwork serpentinites with incipient sulphide mineralisation have undergone a different type of hydrothermal alteration, where talc has extensively replaced serpentine-group minerals forming steatite (soapstone) (Fig. 4d). Oxides like magnetite are rare and relic Cr-spinel grains are highly altered. Trace sulphides may occur. Usually pyrrhotite associated with ISS/Ccp and, more rarely, altered pyrite.

Semi-massive sulphides (SMS)

The semi-massive sulphide unit is the result of the pervasive replacement of stockwork silicates by hydrothermal sulphides. Here, host rock relics may be preserved as extremely altered serpentinite “islands” surrounded by sulphide masses or as altered Cr-spinel relics that prove the ultramafic nature of the host rock (Fig. 4e). Sulphide assemblages are similar to the ones observed in stockwork samples. Anhedral masses of pyrite are sometimes replaced by magnetite II or by ISS/Ccp.

Massive sulphides (MS)

Cu-massive sulphides (Cu-MS) - Cu-massive sulphides are characterized by a dense array of ISS/Ccp sulphides with low porosity and no apparent mineralogical zonation. This unit results from extensive replacement of the pyrite-rich SMS ore by ISS/Ccp. Some sections show annealing (120° joints) indicative of recrystallization processes (Fig. 4f). ISS/Ccp contains altered rims of covellite and rare fracture-filling anhydrite.

Massive sulphide chimneys (MS-ch I, II) - As opposed to Cu-MS, sulphide chimneys are porous and frequently show concentric mineralogical zonation around a vent orifice. Textures correspond to an interlocking network of sulphides representative of open-space type deposition due to mixing of a hot metal-rich vent fluid with cool seawater. Rainbow hydrothermal chimneys are sphalerite-rich (Fig. 4g, h). MS-ch type I are defined by a lower temperature sulphide assemblage composed of euhedral pyrite overprinted by colloform sphalerite with ISS/Ccp intergrowths (Fig. 4g). MS-ch type II contain lamellar crystals of pyrrhotite interlocked with sulphide aggregates. The latter are zoned, with an ISS/Ccp core rimmed by chalcopyrite, both surrounded by colloform sphalerite (Fig. 4h). Textural evaluation of MS-ch type II indicates cogenetic sulphide formation and assemblages that are compatible with high temperature venting.

Rodingitic rocks

A few samples are composed of relics of extremely altered rodingite-like, serpentinised material in a matrix of aragonite, which appears to have extensively replaced former serpentinites. Petrography reveals aggregates of interpenetrating serpentine with rare bastite relics plus chlorite and rare garnet (grossular/hydrogrossular?) surrounded by euhedral grains of aragonite. Large hydrothermal diopside grains that are not in textural equilibrium

with aragonite may overprint the serpentine/chlorite aggregates. These assemblages are indicative of Ca mobilization, following retrograde serpentinisation somewhat similar to the rodingitization processes as described by O'Hanley (1996).

Methodology

Electron microprobe analyses were performed using a CAMECA SX50 with 3 crystal spectrometers at the University of Toronto. Silicates were analysed using an accelerating voltage of 15 kV, and sample current of 15 nA with a beam diameter of 3 microns. The sulphide and oxide routine took place under an accelerating voltage of 20 kV and sample current of 30 nA with a beam diameter of 1 micron. A few serpentine-group minerals were analysed at the University of Lisbon using a JEOL JCXA 733 microprobe. Whole-rock geochemistry analyses were undertaken by ACTLABS, Canada using the LITORESEARCH QUANT package. Procedures for rock pulverization were as follows: (1) selected samples were diamond-sawn into small slices (< 1.5 cm thick), (2) slices were then ground using a diamond-grinding wheel in order to prevent contamination, (3) subsequently samples were carefully washed and dried at 25°C, (4) dried samples were crushed using a hammer while enclosed within thick paper envelopes to prevent metal contamination, (5) small fragments were then powdered in an agate ring mill. For Nd isotope analyses, 100 mg to a few grams of bulk powder samples were dissolved either in a mixture of HCl and HNO₃, or HF and HNO₃ in a 3:1 proportion followed by a second step, in concentrated HNO₃ in a sealed savillex beaker and left on a hotplate at 150°C for a couple of days. The solution was then dried up and converted to chloride form by adding 5 to 10ml of 6 M HCl. Separation of Sm and Nd was done using a routine two column ion-exchange technique which firstly extracts REE through a cation exchange column, followed by a separation of Nd from Sm through a second column packed with Kel-F Teflon coated HDEHP. Nd isotope ratios were measured at the National Oceanography Centre, Southampton, England on a seven-collector VG Sector 54 mass spectrometer. ¹⁴³Nd/¹⁴⁴Nd ratios were determined in multi-dynamic collection mode. Isotope ratios were normalized to ¹⁴⁶Nd/¹⁴⁴Nd = 0.7219. Measured values for JNd-i standards were ¹⁴³Nd/¹⁴⁴Nd = 0.512104 ± 10 (2sd, n = 38).

Results

Rock sample locations and descriptions of representative samples are reported in Table 1. Results for REE, mineral chemistry and Nd isotopic compositions are given in Tables 2, 3 and 4, respectively.

Table 1 Sample location chart with mineralogy and rock type description. Abbreviations: () relics, *Anh* anhydrite, *Arg* aragonite, *Chl* chlorite, *Di* diopside, *ISS/Ccp* exsolved chalcopyrite in intermediate solid solution, *Mgt* magnetite, *Ol* olivine, *Po* pyrrhotite, *Px* pyroxene, *Py* pyrite, *Sp* sphalerite, *Spl* Cr-spinel, *Srp* serpentine-group minerals and *Tlc* talc

Sample	Dredge Start		Dredge Finish		Mineralogy	Rock Type
	Lat	Lon	Lat	Lon		
IR-DR-01-A-05	36°19.2 N	33°54 W	36°16.2 N	33°45 W	(Ol), (Px), (Spl), Srp, Chl, Mgt	Serpentinite
IR-DR-02-B-04	36°16.2 N	33°54 W	36°13.8N	33°45 W	(Spl), Srp, Chl, Mgt	Serpentinite
IR-DR-02-D	36°16.2 N	33°54 W	36°13.8N	33°45 W	(Spl), Srp, Mgt, Py	Stockwork
IR-DR-03-F	36°13.8 N	33°54 W	36°11.4 N	33°45 W	(Spl), Srp, Mgt, Arg	Stockwork
IR-DR-02-C-01	36°16.2 N	33°54 W	36°13.8N	33°45 W	(Spl), Srp, Mgt, Py, ISS/Ccp, Po, Sp, Arg	Stockwork
SH1-DR3-9-4	36°13.8 N	33°54.6 W	36°13.8 N	33°53.4 W	Py, ISS/Ccp, Mgt	Stockwork
SH1-DR3-9-9	36°13.8 N	33°54.6 W	36°13.8 N	33°53.4 W	Py, ISS/Ccp, Mgt	Stockwork
IR-DR-03-E	36°13.8 N	33°54 W	36°11.4 N	33°45 W	(Spl), Tlc, Mgt, Po, ISS/Ccp	Steatite
SH1-DR3-8-3	36°13.8 N	33°54.6 W	36°13.8 N	33°53.4 W	(Spl), Tlc, Mgt, Po, ISS/Ccp	Steatite
IR-DR-01-C-01	36°19.2 N	33°54 W	36°16.2 N	33°45 W	Py, ISS/Ccp, Mgt	Semi-massive sulphide
IR-DR-01-G-02	36°19.2 N	33°54 W	36°16.2 N	33°45 W	(Spl), Py, ISS/Ccp, Mgt	Semi-massive sulphide
SH1-DR3-2-1	36°13.8 N	33°54.6 W	36°13.8 N	33°53.4 W	Py, ISS/Ccp, Mgt	Semi-massive sulphide
SH1-DR3-2-3	36°13.8 N	33°54.6 W	36°13.8 N	33°53.4 W	Py, ISS/Ccp, Po	Semi-massive sulphide
SH1-DR3-1-2	36°13.8 N	33°54.6 W	36°13.8 N	33°53.4 W	ISS/Ccp, Anh	Cu-massive sulphides
IR-DR-02-L-01	36°16.2 N	33°54 W	36°13.8N	33°45 W	Srp, Chl, Arg, Di, Po	Rodingitic material

Bulk-rock geochemistry

Figure 5 illustrates major and trace element variation of 15 selected samples that represent the mineralising sequence from serpentinite to massive sulphides.

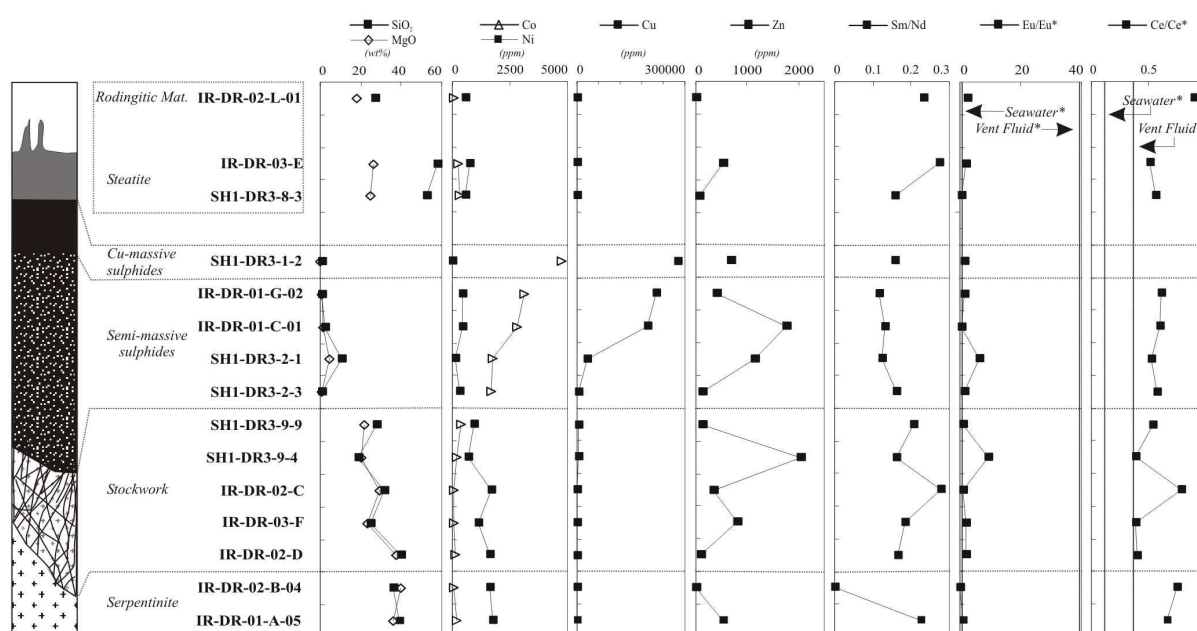


Fig. 5 Bulk-rock chemical data of selected elements (SiO_2 , MgO , Co , Ni , Cu , Zn , Sm/Nd , Eu/Eu^* , Ce/Ce^*)

from representative samples of the upper section of the hydrothermal system

SiO_2 and MgO contents decrease from serpentinites towards stockwork, semi-massive sulphides and massive sulphides, due to gradual silicate destruction with progressive sulphide replacement. Steatites are more silica-rich due to the predominance of talc. Steatites are, at least locally, indicative of higher silica activity and high fluid/rock ratio. Co abundances in the unmineralised serpentinites are below 100 ppm, while Co contents in mineralised samples increase with the amount of sulphide mineralisation, reaching high concentrations in semi-massive sulphides (~2335 ppm Co, n=4), Cu-massive sulphides (~4770 ppm Co) and massive sulphide chimneys (6300 ppm Co) (Marques 2005, Ph.D. thesis in preparation). Ni is absent in Cu-rich massive sulphides and massive sulphide chimneys. Unmineralised serpentinites

are Cu depleted (~95 ppm, n=7) and Cu abundances remain fairly low in the stockwork (~1421 ppm, n=7) and in steatites (~257 ppm, n=3) (Marques 2005, Ph.D. thesis in preparation). In more mineralised rocks, Cu increases sharply and becomes a major element, in semi-massive sulphides (~11.3 wt %, n=4), Cu-rich massive sulphides (27.98 wt %; n=1) and massive sulphide chimneys (8.35 wt %; n=1). Selenium is exclusively present in the samples highly enriched in Cu. The high Cu-values are representative of all the strongly mineralised samples thus, if Rainbow was on land, it would be a high-grade copper deposit. Serpentinised peridotites are Ni-rich with lower Co (~1681 ppm Ni; ~108 ppm Co; n=7) and Co/Ni ratios ~0.06 (Marques 2005, Ph.D. thesis in preparation) matching P-mantle values (McDonough and Sun 1995). With the development of sulphide mineralisation, bulk-rock Co/Ni ratios increase, resulting in stockwork semi-massive and massive sulphides with Co/Ni >1 (Fig. 3). In absolute terms, Ni contents in serpentinite and stockwork decrease while Co increases sharply. The peridotite precursor has high Ni and low Co, therefore it is difficult to explain the final Co/Ni ratios and the extreme Co enrichment in the massive sulphides as resulting solely from an ultramafic source. Zn is absent in most serpentinites and Zn concentrations are rather low with irregular distribution except in Zn-rich chimneys. Sphalerite is the only Zn sulphide found in the Rainbow assemblages thus its presence or absence dictates Zn abundances (Fig. 5).

Zn-rich rocks are characteristic of massive sulphide chimneys (type I and II) and relate to the focused venting at surface where cooler seawater interacts with hotter vent fluid. Chimneys may contain up to 5.12 wt% Zn (e.g., Ms-ch II) (Marques 2005, Ph.D. thesis in preparation). On the contrary, Cu-rich rocks show evidences of sub-seafloor precipitation and recrystallization (Cu-MS) where higher temperatures can be attained. The presence, in these amounts, of Cu, Zn, and Co is characteristic of mafic-hosted seafloor hydrothermal systems. One may expect the contribution of a mafic metal source responsible for Cu, Zn and Co input, along with Fe, into the system.

Table 2 Rare earth element (REE) analysis (in ppm) of serpentinites, stockwork, steatites, rodingitic material, semi-massive sulphides and massive sulphides from the Rainbow vent field. (n.d). not detected

Sample	IR-DR-01-A-05	IR-DR-02-B-04	IR-DR-02-D	IR-DR-03-F	IR-DR-02-C	SH1DR-3-9-4	SH1DR-3-9-9	SH1DR-3-2-3	SH1DR3-2-1	IR-DR-01-C-01	IR-DR-01-G-02	SH1DR-3-1-2	SH1DR-3-8-3	IR-DR-03-E	IR-DR-02-L-01	BIR-1	BIR-1	DNC-1	DNC-1
Type	Serp	Serp	St	St	St	St	St	SMS	SMS	SMS	SMS	Cu-MS	Stea	Stea	Rod	measured	certified	measured	certified
La	1.03	0.07	1.10	1.03	0.21	2.08	1.39	7.36	21.46	19.23	2.39	0.21	2.13	0.48	0.64	0.81	0.62	3.91	3.8
Ce	1.46	0.09	0.80	0.73	0.33	1.50	1.39	7.80	20.27	21.27	2.66	0.43	2.17	0.45	1.18	2.11	1.95	8.59	10.6
Pr	0.28	0.01	0.11	0.12	0.03	0.20	0.16	0.56	1.23	1.47	0.19	0.05	0.15	0.04	0.12	0.39	0.38	1.04	1.3
Nd	0.93	<0.05	0.30	0.27	0.13	0.52	0.44	1.78	3.54	4.54	0.57	0.16	0.45	0.11	0.47	2.52	2.5	4.95	4.9
Sm	0.21	0.01	0.05	0.05	0.04	0.08	0.09	0.28	0.44	0.60	0.07	0.03	0.07	0.03	0.11	1.13	1.1	1.43	1.38
Eu	0.09	0.01	0.04	0.03	0.01	0.26	0.03	0.1	0.81	0.05	0.03	0.01	0.01	0.02	0.11	0.55	0.54	0.62	0.59
Gd	0.25	<0.01	0.08	0.05	0.03	0.09	0.09	0.18	0.32	0.36	0.05	0.02	0.05	0.04	0.15	1.86	1.85	2.05	2
Tb	0.04	<0.01	0.01	<0.01	<0.01	<0.01	<0.01	0.02	0.06	0.05	<0.01	<0.01	<0.01	0.01	0.03	0.39	0.36	0.41	0.41
Dy	0.26	0.01	0.08	0.04	0.04	0.07	0.07	0.09	0.29	0.16	0.02	0.02	0.05	0.06	0.18	2.65	2.5	2.73	2.7
Ho	0.06	<0.01	0.02	<0.01	<0.01	<0.01	<0.01	0.01	0.06	0.02	<0.01	<0.01	<0.01	0.01	0.04	0.55	0.57	0.59	0.62
Er	0.18	0.01	0.05	0.02	0.02	0.05	0.05	0.02	0.17	0.04	<0.01	0.01	0.04	0.05	0.13	1.84	1.7	2.02	2
Tm	0.03	<0.005	0.01	<0.005	<0.005	<0.005	0.005	<0.005	0.02	<0.005	<0.005	<0.005	0.05	0.01	0.02	0.29	0.26	0.32	(0.33)
Yb	0.18	0.03	0.05	0.02	0.04	0.02	0.03	0.01	0.13	0.02	<0.01	<0.01	0.03	0.05	0.13	1.65	1.65	1.93	2.01
Lu	0.03	0.004	0.01	0.004	0.005	0.004	0.005	0.003	0.02	<0.002	<0.002	<0.002	0.01	0.01	0.02	0.26	0.26	0.31	0.32
(Eu/Eu*) _N	1.17	-	1.88	1.83	1.22	9.15	0.88	1.32	6.55	0.35	1.47	1.44	0.26	1.85	2.52				
(Ce/Ce*) _N	0.75	0.99	0.49	0.48	0.93	0.49	0.66	0.73	0.67	0.76	0.77	1.13	0.71	0.65	1.03				
(La/Yb) _N	3.89	1.59	14.95	34.99	3.79	58.7	29.11	351.5	108.6	650.5	-	-	47.53	6.52	3.34				

Rare earth element (REE) concentrations measured in representative rock samples are listed in Table 2. Chondrite-normalized REE patterns are plotted in Fig. 6. With one exception, europium anomalies (Eu/Eu*) are higher than in seawater, but still below those of the vent fluid (Fig. 5). Apart from three samples, most of the mineralised rocks display relevant positive Eu anomalies (1.22 to 9.15), suggesting interaction with hydrothermal fluids. Serpentinites, stockwork and steatites present flat HREE normalised values at about chondrite abundances. Serpentinites show a nearly flat LREE pattern, parallel to seawater with a weak Ce negative anomaly (Fig. 6a). Stockwork samples depict LREE enrichment over HREE, somewhat comparable to vent fluid REE patterns, with a slight negative Ce anomaly (Fig. 6b). REE patterns of semi-massive sulphides clearly reflect the vent fluid REE pattern with significant LREE enrichment and positive Eu anomalies. Cu-rich massive sulphides are REE depleted (Fig. 6d). Steatite and rodingitic material show LREE patterns similar to stockwork, but with no Ce anomaly (Fig. 6c).

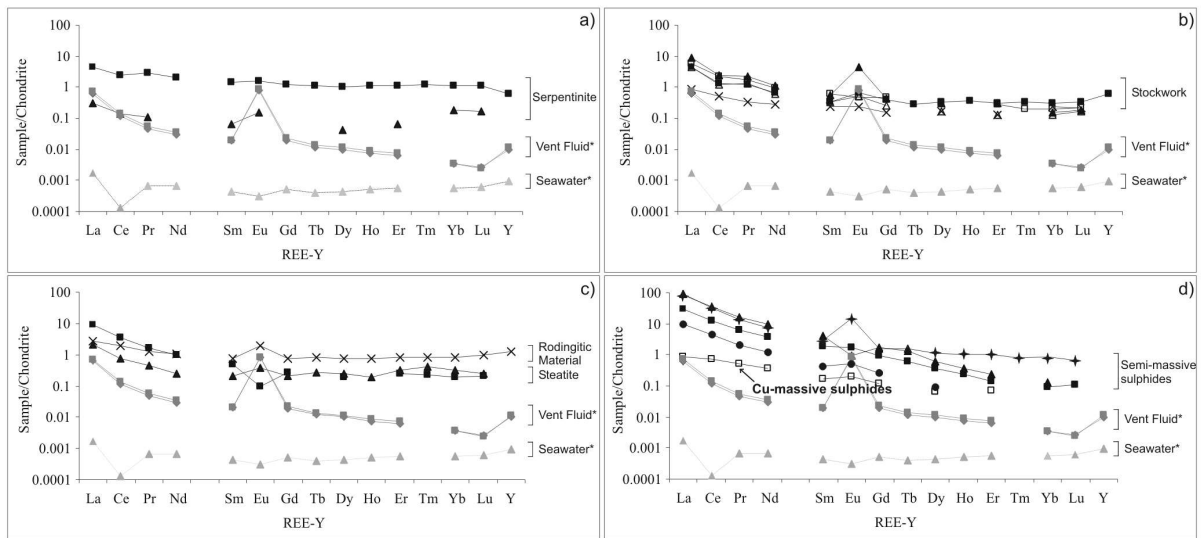


Fig. 6 Chondrite normalized REE patterns for selected representative Rainbow vent field rocks. **a** Serpentinites.

b Stockwork. **c** Steatite and rodingitic material. **d** semi-massive and massive sulphides. Data in Table 3.

Normalising values after McDonough and Sun (1995) *Rainbow vent fluid data (x10) and seawater data (x100)

after Douville et al. (2002)

Mineral Chemistry

438 microprobe analyses were completed, 308 of them in sulphides. Chemical compositions of pyrite, pyrrhotite, ISS/Ccp and sphalerite from the different rock types are reported in Table 3.

Table 3 Electron microprobe analyses (average values in wt%) of pyrite, pyrrhotite, ISS/Ccp and sphalerite from the Rainbow vent field. Abbreviations: *N* number of microprobe analyses, (-) not detected, *SMS* semi-massive sulphides, *MSch I-II* massive sulphide chimneys type I and II, *Py* pyrite, *ISS/Ccp* intermediate solid solution with exsolved chalcopyrite lamellae, *Po* Pyrrhotite, *Sp* sphalerite and *Marm* marmatite

Mineral	Lithology		Fe	Cu	S	Ag	Zn	Cd	Ni	Co	Total	N
Pyrite	Early Stock work		43.6	-	50.5	-	-	-	3.46	0.10	97.8	3
	Stock work		46.3	-	52.9	-	0.01	-	0.32	0.03	99.5	34
	Steatite		46.2	0.01	53.2	0.01	0.01	-	0.02	0.20	99.6	8
	SMS		46.4	0.10	53.3	0.01	0.04	0.01	0.03	0.18	100.1	45
	MSch I		45.3	-	52.5	-	0.30	-	-	0.12	98.26	4
Pyrrhotite	Stockwork		59.7	0.01	39.4	0.01	0.03	0.03	0.38	0.04	99.58	19
	Steatite		59.8	0.11	38.6	0.01	0.02	0.02	0.10	0.33	99.04	8
	SMS		60.9	0.02	38.4	0.02	0.02	0.03	0.11	0.06	99.55	24
	MSch II		59.6	0.02	38.8	0.02	0.19	0.02	0.01	0.40	99.09	3
ISS/Ccp	Stockwork	<i>ISS</i>	40.7	22.3	35.7	0.02	0.66	0.03	0.26	0.09	99.71	8
		<i>Ccp</i>	31.0	33.6	35.5	0.03	0.36	0.02	0.13	0.03	100.6	9
	Steatite	<i>ISS</i>	39.7	23.9	35.0	0.01	0.19	0.02	0.05	0.41	98.39	4
		<i>Ccp</i>	32.3	29.9	34.6	0.01	0.21	0.03	0.03	0.22	98.70	3
	SMS	<i>ISS</i>	40.8	20.4	37.7	0.01	0.31	0.03	0.07	0.07	99.39	11
		<i>Ccp</i>	32.3	32.3	35.2	0.01	0.13	0.02	0.04	0.20	100.2	30
	Cu-MS	<i>ISS</i>	39.2	24.7	35.4	0.01	0.03	0.02	0.01	0.52	100.0	13
	MSch I	<i>Ccp</i>	30.8	33.1	34.8	0.02	1.21	0.02	0.01	0.02	99.98	5
	MSch II	<i>ISS</i>	42.2	21.7	36.0	0.03	0.16	0.01	-	0.34	100.4	8
		<i>Ccp</i>	34.5	29.9	35.3	0.07	0.24	0.06	0.02	0.18	100.2	1
Sphalerite	Stockwork	<i>Marm.</i>	13.4	0.04	33.7	0.01	52.9	0.11	0.01	0.01	100.2	20
		<i>Sp.</i>	3.15	0.05	33.0	0.00	63.2	0.12	0.01	0.00	99.60	10
	MS-ch type I	<i>Marm.</i>	10.7	0.90	32.6	0.07	53.5	0.33	-	0.05	98.16	5
		<i>Sp.</i>	1.40	0.22	31.8	0.10	62.8	0.06	-	0.01	96.45	5
	MS-ch type II	<i>Marm.</i>	15.6	0.36	34.9	0.01	49.7	0.09	-	0.27	99.95	3

Fe/S ratios in pyrite are fairly constant except in the early stockwork where pyrite is Ni-rich, containing up to 3.46 wt% Ni and 0.1 wt% Co. Fig. 7 illustrates the Co and Ni variation in pyrite minerals from the Rainbow vent field. Stockwork contains Ni-rich pyrite whose Ni contents decrease gradually towards the semi-massive sulphides and massive sulphide chimneys. In contrast, low Co concentrations found in stockwork pyrite increase towards the semi-massive sulphides and massive sulphide chimneys. Hence, pyrite from stockwork has Co/Ni < 1 and the remaining pyrites from the semi-massive sulphides, massive

sulphide chimneys and steatites are Co-rich with $\text{Co/Ni} > 1$. Similar Co/Ni ratio variation is observed for pyrrhotite, ISS/Ccp and sphalerite with the exception that pyrrhotite from semi-massive sulphides still reveals $\text{Co/Ni} < 1$.

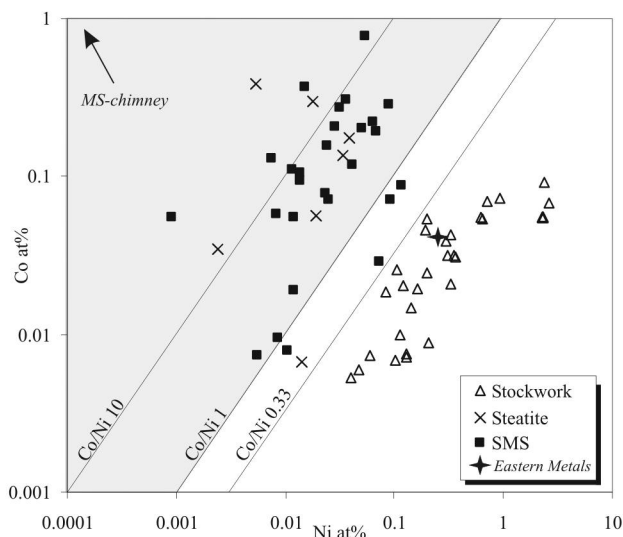


Fig. 7 Co versus Ni (at %) plot for pyrite from the Rainbow vent field. Pyrite from MS-ch I is not represented since Ni is absent. The black star represents the average value of pyrite from the serpentinite-hosted Eastern Metals deposit (Auclair et al. 1993). The compositional field where $\text{Co/Ni} > 1$ (shaded area) delimits pyrites of volcanogenic association (VMS) (Loftus-Hills and Solomon 1967; Bralía et al. 1979; Mookherjee and Philip 1979; Walshe and Solomon 1981; Bajwah et al. 1987; Lawrie and Miller 2000)

ISS/Ccp chemistry is complex, although comparable to that of the Bent Hill and ODP mounds on the Juan de Fuca Ridge (Lawrie and Miller 2000). Fe and Cu proportions vary widely (Fe ~ 42.16 wt% to ~ 30.75 wt%, Table 4) due to chalcopyrite exsolution lamellae. These non-stoichiometric concentrations suggest that no equilibrium has been attained in the newly formed sulphides. Zn contents in the chalcopyrite portions are variable, ~ 0.36 wt% in St, ~ 0.13 wt% in SMS, ~ 1.21 wt% MS-ch I, ~ 0.24 wt% MS-ch II and 0.21 wt% Stea. The same defines the ISS portion which contains ~ 0.66 wt% in St, ~ 0.31 wt% in SMS, 0.03 wt% in Cu-MS, 0.16 wt% in MS-ch II and 0.19 wt% in Stea. Experimental work by Kojima and Sugaki (1985) simulating hydrothermal conditions for the Cu-Fe-Zn-S system between 300°C

and 500°C and pressures of 500kg/cm², confirmed that the Zn content of ISS and chalcopyrite decreases with decreasing temperature, as previously observed by Hutchinson and Scott (1981). If we consider either of the main mineralising sequences, St – SMS – MS-ch II and St – Stea, Zn contents in ISS/Ccp decrease upwards, which suggests a decrease in temperature, as is to be expected. This does not apply to Cu-MS and MS-ch I units. The first, which is Zn-free, probably results from recrystallization and zone refining inducing Zn remobilisation, whereas Ccp in MS-ch I shows anomalously high Zn contents, possibly due to small sphalerite inclusions. Because ISS can easily turn into chalcopyrite, the regular presence of ISS in Rainbow indicates rapid cooling with effective sealing (Kase et al. 1990). There are two distinct populations of sphalerite according to FeS contents. Lower FeS values (2.9 to 3.4 wt% in St and 2.45 to 0.9 wt% in MS-ch I) correspond to sphalerite_{ss} associated with pyrite. High FeS values (10.41 to 17.9 wt% in St to 14.41 to 17.29 wt% in MS-ch II) correspond to sphalerite (marmatite), related to pyrrhotite – ISS/Ccp assemblages. Low FeS in sphalerite suggests increasing sulphur activity (a_{S_2}), decreasing temperature, or the combination of both (Vaughan and Craig 1997). Marmatite (Cu-rich) occurs in MS-ch I associated with ISS/Ccp (Zn-rich), suggesting the presence of minute inclusions of ISS/Ccp within marmatite and interference during analytical processes. Sphalerite specimens from sulphide chimneys contain relevant amounts of Cu, Ag and Cd (MS-ch I) or Cu and Co (MS-ch type II). Variation in the FeS contents from sphalerite, if in equilibrium with pyrite or pyrrhotite, suggest that their precipitation occurred under different conditions, most probably at different temperatures. This may reflect different degrees of mixing of hotter vent fluid with cold seawater on proximal and distal areas of the hydrothermal system.

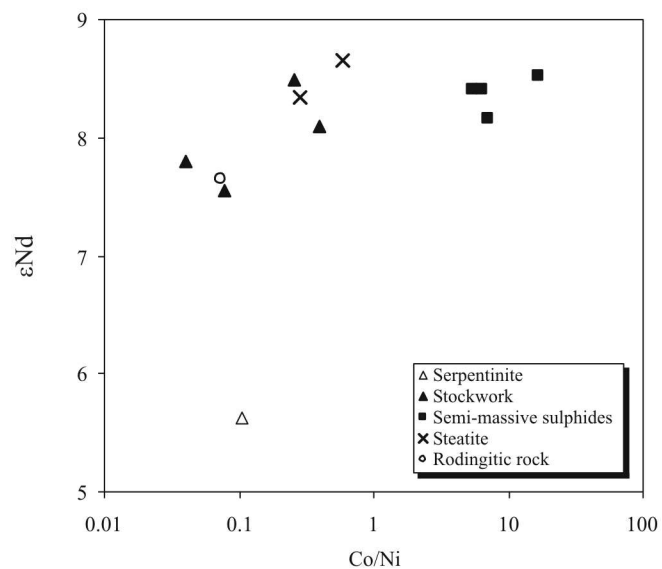
Nd isotopes

Radiogenic isotopes are powerful tools for identifying sources and processes, and will be used in conjunction with trace element data to identify the fluid source(s). The Nd isotope compositions of 12 samples from the Rainbow sulphide deposit are reported in Table 4 and plotted against Co/Ni and 1/Nd in Figs. 8 and 9. The high Nd (and REE) concentrations of the semi-massive sulphides compared with the other mineralised samples are, most probably, related to the occurrence of phyllosilicates since REE are not easily incorporated in sulphides. This would also explain the REE-depletion in silicate-free massive sulphides (Table 2).

$^{143}\text{Nd}/^{144}\text{Nd}$ ratios of all samples, apart from serpentinite, vary in a narrow range between 0.513025 and 0.513082, corresponding to a ϵ_{Nd} of +7.55 to +8.66. Unmineralised serpentinite, however, presents a very distinctive Nd isotopic composition at 0.512926 ($\epsilon_{\text{Nd}} = +5.62$). This serpentinite exhibits the lowest ϵ_{Nd} and Co/Ni ratio for 1/Nd equal to 1. Stockwork samples exhibit low Co/Ni ratios (Co/Ni < 1) and increasing ϵ_{Nd} values (+7.55 - +8.52) and 1/Nd ratios (1.91 to 8) while the semi-massive sulphides show very uniform ϵ_{Nd} values between +8.15 and +8.52 and high Co/Ni ratios (Co/Ni > 5) and variable 1/Nd ratios (0.22 - 1.75) (Fig. 8). Rodingitic material and part of the stockwork exhibit lower ϵ_{Nd} and Co/Ni values when compared to the semi-massive sulphides.

Table 4 Nd isotope data from representative samples of the Rainbow vent field

Sample	Rock type	Nd (ppm)	1/Nd	$^{143}\text{Nd}/^{144}\text{Nd}$	$\pm 2\text{sE}$	ϵ_{Nd}
IR-DR-02-L-01	Rodingitic Material	0.47	2.13	0.513030	16	7.65
IR-DR-03-E	Steatite	0.11	9.09	0.513066	53	8.35
SH1-DR3-8-3	Steatite	0.45	2.21	0.513082	16	8.66
IR-DR-01-G-02	Semi-massive sulphide	0.57	1.75	0.513056	8	8.15
IR-DR-01-C-01	Semi-massive sulphide	4.52	0.22	0.513069	8	8.41
SH1-DR3-2-1	Semi-massive sulphide	3.54	0.28	0.513075	6	8.52
SH1-DR3-2-3	Semi-massive sulphide	1.78	0.56	0.513069	9	8.41
SH1-DR3-9-9	Stockwork	-	-	0.513053	15	8.10
SH1-DR3-9-4	Stockwork	0.52	1.91	0.513073	6	8.49
IR-DR-02-C	Stockwork	0.13	8.00	0.513075	55	8.52
IR-DR-03-F	Stockwork	0.30	3.33	0.513025	26	7.55
IR-DR-01-A-05	Serpentinite	0.93	1.08	0.512926	6	5.62

**Fig. 8** ϵ_{Nd} versus bulk-rock Co/Ni ratios in selected samples from the Rainbow vent field

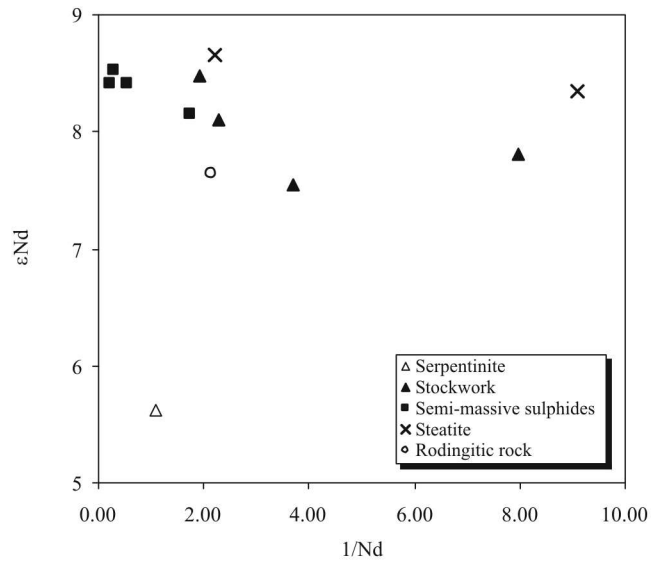


Fig. 9 ϵ_{Nd} versus $1/Nd$ in selected samples from the Rainbow vent field.

Discussion

Serpentinisation and heat generation

Serpentine textures and mineralogy reveal that serpentinisation has taken place sub-seafloor under low-temperature retrograde metamorphism. Olivine reacted first, and more extensively than pyroxene, producing pseudomorphic (lizardite-dominated) textures. Considering the latter observations, temperatures were certainly below 350°C (Moody 1976; Janecky and Seyfried 1986) and probably under 270°C (O'Hanley 1996; Allen and Seyfried 2004). Serpentinisation reactions are exothermic (MacDonald and Fyfe 1985; Fyfe 1992; O'Hanley 1992; Kelley et al. 2001; Lowell and Rona 2002; Schroeder et al. 2002; Allen and Seyfried 2004) but are unlikely to produce hydrothermal temperatures above a few tens of degrees Celsius. In order to produce hydrothermal fluids slightly above 100°C, serpentinisation rates need to be extremely high (100 Kg/s) and flow rates low (10 Kg/s) (Lowell and Rona 2002). At the Rainbow the opposite occurs: flow rates are high (500Kg/s) and serpentinisation rates are probably low (~ 0.1 Kg/s) except when, episodically, new reaction surfaces are available (MacDonald and Fyfe 1985; Thurnherr and Richards 2001; Lowell and Rona 2002). Thus, it is extremely unlikely that serpentinisation reactions alone can produce the reported high temperatures at the Rainbow vents. Furthermore, the hydrothermal sulphide mineralisation event indisputably overprints the serpentinisation event thus any considerations regarding the vent fluid properties cannot be directly attributed to serpentinisation reactions alone. Consequently, the presence of a magmatic heat source at depth as previously proposed by several authors (Cave et al. 2002; Lowell and Rona 2002; Mével et al. 2003; Allen and Seyfried 2004) prevails as a reasonable explanation.

Sulphide mineralisation

Serpentinites are naturally Cu and Zn depleted but the textures and chemistry of the sulphide-bearing rocks found at Rainbow show conspicuous similarities with mafic VMS deposits. Accordingly, the Rainbow massive sulphide ore-grade deposit is Cu and Zn-rich (28 wt% Cu; 5 wt% Zn), but Pb depleted whereas the upper parts of the hydrothermal system are also extremely Co-enriched (up to ~6300 ppm) with high Co/Ni ratios. These elements are characteristic of mafic-hosted seafloor hydrothermal systems. It is reasonable to assume that a mafic metal source is responsible for Cu, Zn and Co input, along with Fe, into the system. Cu-Fe sulphide chemistry data suggest that temperature decreases from deeper stockwork through sub-surface semi-massive sulphides to massive-sulphide chimneys.

Ni and Co are remobilised, during serpentinisation, from primary minerals into serpentinite-group minerals and later, during sulphide mineralisation, into sulphides (Marques et al. 2003). While Ni gradually decreases, Co increases sharply with the evolution of the hydrothermal system (Srp-St-Stea and Srp-St-SMS-MS) indicating Co input. These observations apply both to bulk-rock and sulphide chemistry data. Co/Ni ratios have been used as indicators discriminating sulphide deposits of different settings. At Rainbow, Co/Ni ratios found in stockwork pyrite compare well to those of pyrites from the serpentinite-hosted Eastern Metals deposit (Auclair et al. 1993) whereas the Co-rich pyrite with Co/Ni ratios >1 , found in semi-massive and massive sulphides, match those of volcanogenic pyrite found in VMS deposits from different localities (Loftus-Hills and Solomon 1967; Bralía et al. 1979; Mookherjee and Philip 1979; Walshe and Solomon 1981; Bajwah et al. 1987). Similar Co/Ni ratio variation has been pointed out in the Outokumpu deposit ores, with Co/Ni ratios typical of VMS deposits except for a few Ni-rich pyrites found in the deeper parts of the deposit, which have been interpreted as earlier sulphides (Loukola-Ruskeeniemi 1999).

In the Rainbow vent field, Co/Ni ratios seem to be excellent tools for discriminating between the various units.

LREE enrichment occurs alongside sulphide mineralisation reaching a maximum in semi-massive sulphides and decreasing again in the massive sulphide units. The presence of altered serpentinite relics in semi-massive sulphides may favour the observed LREE retention. The REE-depleted character of the unmineralised serpentinites and the increasingly LREE enrichment in the sulphide bearing rocks strongly suggest that the source of metals (Cu, Zn and Fe) transported by the hydrothermal fluid, should also contribute with LREE. HREE patterns are nearly constant throughout the system compatible with the higher LREE mobility as Cl complexes in acidic solutions (Mills and Elderfield 1995; Douville et al. 1999).

Nd isotopes

Hydrothermal fluids that were originally seawater have been progressively modified via (direct or indirect) magmatic interactions during percolation. The sulphides formed during the hydrothermal sulphide mineralisation episode acquired the Nd isotopic signature of the hydrothermal fluid from which they derived. From the above sections, there is clear evidence that the sulphide-bearing serpentinites (stockwork and semi-massive sulphides) and related rocks (steatites and rodingitic material) result from the same peridotite precursor as the serpentinite. However, it is the combination of the serpentinisation process with the presence of a magmatic heat source at depth (e.g. intrusion of a gabbroic body) that may explain the chemical characteristics of the Rainbow site (Cave et al. 2002; Lowell and Rona 2002; Mével et al. 2003; Allen and Seyfried 2004). The contribution of two sources (seawater and magmatic) in the hydrothermal fluid at Rainbow is also supported by Nd isotopic compositions and Co/Ni and 1/Nd ratios (Fig. 8, 9).

At the Rainbow vent field, mineralised samples are characterised by ϵ_{Nd} values of +7.55 to +8.66, but no Nd isotope ratios have, so far, been measured on Rainbow hydrothermal fluids. Basalts in the vicinity of the Rainbow vent site (South AMAR segment

between 36.29°N and 35.67°N) exhibit ϵ_{Nd} values at +8.56 to +9.95 ($^{143}Nd/^{144}Nd = 0.513077 - 0.513148$) which correspond to the top end of our sample variation range (Fig. 8, 9; Dosso et al. 1999). In contrast, the present day deep-water circulation in the Rainbow rift valley is characterized by an inflow of North East Atlantic Deep Water, from the eastern ridge flank, with ϵ_{Nd} value of -12.4 (Thurnherr and Richards 2001; Thurnherr et al. 2002; Lacan 2002). In comparison, the East Pacific Rise (EPR) hydrothermal fluids present ϵ_{Nd} values of +5 to +7 (Michard and Albarede 1986) lower by 2 ϵ_{Nd} values than those of the oceanic crust at that location. Mineralised rocks and oceanic crust from the Rainbow area exhibit similar ϵ_{Nd} variations to the EPR, contrasting with the Nd isotope signature of the seawater within the area.

The low ϵ_{Nd} value of the unmineralised serpentinite probably results from simple peridotite-seawater interaction as supported by the low Co/Ni ratio (low Co/Ni ratio in peridotite and seawater, *see* Niu et al. 2001). Subsequently, a higher temperature hydrothermal fluid with high Co/Ni ratios and radiogenic Nd isotopic composition is gradually superimposed on the previous regime. This leads to the formation of sulphide mineralisation during focused fluid upflow, mainly under the seafloor. This would explain the mixing trend in the stockwork samples and rodingitic material that preserve characteristics of the earlier serpentinitisation-related fluid regime (low Co/Ni, unradiogenic Nd isotope), mixed with the later mineralising fluid regime (high Co/Ni, radiogenic Nd isotopic composition). The non-mixing trend in the semi-massive sulphides is generated by the high ϵ_{Nd} and Co/Ni values and low 1/Nd. The emplacement of a gabbroic body (with N-MORB affinity) within the serpentinites can provide heat and elements which easily explain the isotope signatures and all other peculiarities found in the Rainbow vent field.

Vent fluid chemistry

Rainbow fluids hold the highest reported chloride concentration, the lowest end-member pH, high trace metal contents and high REE, K, Rb and Cs contents (Douville et al. 2002). Experiments on simple peridotite-seawater interactions at temperatures below 350°C produced high pH fluids (neutral to alkaline), rich in H₂, CH₄, H₂S, Mn and SiO₂ with low dissolved metal contents (Seyfried and Dibble 1980, Berndt et al. 1996; Donval et al. 1997; Charlou et al. 1997; Kelley et al. 2001; Palandri and Reed 2004). At temperatures of ~400°C, fluids are initially acidic (pH increasing afterwards) with high dissolved Fe, Ca and SiO₂ (Seyfried and Ding 1995; Allen and Seyfried 2003, 2004, 2005). Furthermore, Wetzel and Shock (2000) have calculated that simple peridotite-seawater interaction would produce a fluid with less than 50% K and ~95% SiO₂ than the fluid resulting from basalt-seawater reactions. These experiments could not reproduce the chemistry of the Rainbow vent fluids, most likely because they were based on the assumption that serpentinisation occurs at high temperatures, with olivine stable over pyroxene and antigorite as the stable serpentine phase.

On the other hand, experiments on basalt-seawater interactions, at ~400°C, produced a low pH fluid, rich in metals (Fe > Mn > Zn > Cu.), H₂S, LREE (La, Ce and Eu) and CaO (Seyfried et al. 1986; Bischoff and Rosenbauer 1989; Bienvendu et al. 1990; Seewald and Seyfried 1990; Palandri and Reed 2004). These results are comparable to the composition of vent fluids from modern basalt-hosted high temperature systems and, remarkably, to the Rainbow vent field (Douville et al. 2002; James et al. 1995; Seewald and Seyfried 1990).

High mFe/mCu and mFe/mMn coupled with high Fe contents in the Rainbow vent fluids are indicative of reducing, acidic and high temperature conditions at the sub-seafloor reaction zone. However Zn content in fluids at temperatures >200°C do not seem to be temperature dependent (Seewald and Seyfried 1990; Large 1992; Hannington et al. 1995; Seyfried and Ding 1995; Charlou et al. 2000; Douville et al. 2002; Allen and Seyfried 2003). Thus the profusion of Zn in the Rainbow fluids is most probably related to source rock composition and/or brine/seawater mixing since there is no evidence for sphalerite

dissolution (Metz and Trefry 2000; Douville et al. 2002). The presence of Co is related to high temperature Cu-rich VMS deposits or even lower temperature fluids, if chlorinity is high (e.g. Besshi-type VMS; Peter and Scott 1997).

The Rainbow end-member fluid is chlorine-rich (750mM Cl) - surpassing seawater chlorinity (546mM Cl) (Douville et al. 2002). The critical point for seawater is 407°C and 298.5 bars (Bischoff and Rosenbauer 1988) indicating that the Rainbow fluids, venting at 365°C and 2400 m depth, have crossed the two-phase boundary below the critical point at minimum temperatures of 380°C (Charlou et al. 2000; Douville et al. 2002). Under sub-critical conditions, boiling seems to be the predominant phase separation process causing the exsolution of volatile components (CO₂, H₂S, CH₄, SO₂, H₂) into the vapour phase, with drastic changes in the pH and fO_2 of the system (Drummond and Ohmoto 1985). Sub-critical boiling results in only moderate increase in salinity (Charlou et al. 2000), which is possibly not enough to explain the high-chlorinity values at Rainbow. Under these conditions, mixing with a high salinity brine or the direct magmatic contribution of a Cl-rich metal-bearing aqueous fluid would explain the high salinities and enriched metal contents.

Conclusions

Textural evidence of sub-seafloor hydrothermal replacement at the Rainbow vent field are indicative of a highly efficient process of trapping metals, essential for the formation of an ore-grade deposit under the seafloor. The new geochemical data, combined with the current knowledge at Rainbow, presents compelling evidence for the presence of a gabbroic intrusion at depth, contributing heat, metals and other elements. The evolution of the system may be summarized as follows:

- (1) A hot gabbroic body has intruded (near) a completely serpentinised peridotite
- (2) The resulting reaction zone is characterized by high temperature, acidic and reducing conditions favouring metal leaching and efficient metal transport by Cl-rich hydrothermal fluids.
- (3) The gabbroic body contributes heat and metals to sustain the hydrothermal circulation and provide the mafic VMS character of the sulphide deposit.
- (4) Strongly positive CH_4 anomalies represent contributions from secondary peridotite-seawater reactions in the surrounding areas.

Acknowledgments

The authors wish to thank Claudio Cermignani (University of Toronto) for technical and analytical support with the EPMA, and Prof. Martin Sinha (NOC), Gabriela Henriques and Yannick Beaudoin for improving the English. The manuscript benefited significantly from constructive comments and suggestions from Bernd Lehmann. Fundação Para a Ciência e Tecnologia (FCT) provided funds for the study through Project SEAHMA (FFCUL/FCT-PDCTM/ P/MAR/ 15281/ 1999) and a Ph.D. scholarship (SFRH/BD/2978/2000) given to A.F.A. Marques. A.F.A. Marques also benefited from a student research grant from the Society of Economic Geologists Foundation. V. Chavagnac was funded by the 2000 National Oceanography Centre, Southampton Research Fellowship. The NERC core strategic science funds the hydrothermal research at NOCS.

References

- Allen D, Seyfried Jr WE (2003) Alteration and mass transfer in the MgO-CaO-FeO-Fe₂O₃-SiO₂-Na₂O-H₂O-HCl system at 400°C and 500 bars: Implications for pH and compositional controls on vent fluids from ultramafic-hosted hydrothermal systems at mid-ocean ridges. *Geochim Cosmochim Acta* 67: 1531-1542
- Allen D, Seyfried Jr WE (2004) Serpentinization and heat generation: Constraints from Lost City and Rainbow hydrothermal systems. *Geochim Cosmochim Acta* 67: 1347-1354
- Allen D, Seyfried Jr WE (2005) REE controls in ultramafic hosted MOR hydrothermal systems: An experimental study at elevated temperature and pressure. *Geochim Cosmochim Acta* 69: 675-683
- Alt JC (1995) Subseafloor processes in the mid-ocean ridge hydrothermal systems. In: Humphris SE, Zierenberg RA, Mullineaux LS, Thomson RE (eds) *Seafloor hydrothermal systems: Physical, chemical, biological and geological interactions* (Geophysical Monograph 91) American Geophysical Union, pp 85-113
- Alt JC, Shanks WC (2003) Serpentinization of abyssal peridotites from the MARK area, Mid-Atlantic Ridge: Sulfur geochemistry and reaction modelling. *Geochim Cosmochim Acta* 67: 641-653
- Auclair M, Gauthier M, Trottier J, Jébrak M, Chartrand F (1993) Mineralogy, geochemistry, and paragenesis of the Eastern Metals serpentinite-associated Ni-Cu-Zn deposit, Quebec Appalachians. *Econ Geol* 88: 123-138
- Baker ET, German CR (2004) On the global distribution of mid-ocean ridge hydrothermal vent-fields. In: German CR, Lin J, Parson LM (eds) *The thermal structure of the oceanic crust and the dynamics of seafloor hydrothermal circulation* (Geophysical Monograph 148) American Geophysical Union, pp 245-266
- Barrie CT, Hannington MD (1997) Introduction: Classification of VMS deposits based on host rock composition. In: Barrie CT, Hannington MD (eds) *Volcanic-associated massive sulfide deposits: Processes and examples in modern and ancient settings*. Ottawa, Society of Economic Geologists 8, pp 1-12
- Barriga FJAS, Costa IMA, Relvas JMR, Ribeiro A, Fouquet Y, Ondreas H, Parson L, FLORES scientific party (1997) The Rainbow serpentinites and serpentinite-sulphide stock work (Mid-Atlantic Ridge, AMAR segment): a Preliminary report of the FLORES results. *EOS Abst* 78: 832

Barriga FJAS, Fouquet Y, Almeida A, Biscoito M, Charlou JL, Costa RLP, Dias A, Marques AMSF, Miranda JM, Olu K, Porteiro F, Queiroz M (1998) Discovery of the Saldanha Hydrothermal Field on the FAMOUS Segment of the MAR (36° 30' N). AGU Fall Meeting 1998, EOS Abst 79(45):F67

Barriga FJAS, Dias A, Marques AFA, Relvas JMRS, Miranda JM, Queiroz G, Lourenço N, Ferreira A, Fouquet Y, Iyer S and the Saldanha and Seahma1 teams (2004) Mount Saldanha revisited: Low-temperature methane discharge through a sediment-capped serpentinite protrusion (MoMAR Area, Mid-Atlantic Ridge, 36°30'N). In: EGU 1st General Assembly, Nice, France, 25 - 30 April 2004

Batuyev BN, Krotov AG, Markov VF, Cherkashev G, Krasnov SG, Lisitsyn Y (1994) Massive sulfide deposits discovered and sampled at 14°45'N, Mid-Atlantic Ridge. BRIDGE newsletter 6: 6-10

Bralia A, Sabatini G, Troja F (1979) A re-evaluation of the Co/Ni ratio in pyrite as geochemical tool in ore genesis problems. *Miner Deposita* 14: 353-374

Berndt ME, Allen DE, Seyfried Jr WE (1996) Reduction of CO₂ during serpentinization of olivine at 300° and 500 bar. *Geology* 24(4): 351-354

Bischoff JL, Rosenbauer RJ (1989) Salinity variations in submarine hydrothermal systems by layered double-diffusive convection. *J Geol* 97: 613-623

Brill BA (1989) Trace-element contents and partitioning of elements in ore minerals from the CSA Cu-Pb-Zn deposit, Australia. *Can Mineral* 27: 263-274

Bogdanov Y, Sagalevitch AM, Chernayev ES, Ashadze AM, Gurvich EZ, Lukashin VN, Ivanov GV, Peresypkin VN (1995) A study of the hydrothermal field at 14°45'N on the Mid-Atlantic Ridge using the "MIR" submersibles. BRIDGE newsletter 9: 9-13

Cave RR, German C, Thomson J, Nesbitt RW (2002) Fluxes to sediments underlying the Rainbow hydrothermal plume at 36°14'N on the Mid-Atlantic Ridge. *Geochim Cosmochim Acta* 66: 1905-1923

Charlou JL, Donval JP, Douville E, Jean-Baptiste P, Radford-Knoery J, Fouquet Y, Dapoigny A, Stievenard M (2000) Compared geochemical signatures and the evolution of Menez Gwen (37°50'N) and Lucky Strike (37°17'N) hydrothermal fluids, south of the Azores triple junction on the Mid-Atlantic Ridge. *Chem Geol* 171: 49-75

Chavagnac V, German C, Milton A, Palmer MR (2005) Sources of REE in sediment cores from the Rainbow vent site (36°14'N, MAR). *Chem Geol* 216: 329-352

Cook NJ (1996) Mineralogy of the sulphide deposits at Sulitjelma, northern Norway. *Ore Geol Rev* 11: 303-338

Costa I (2005) Serpentinization on the Mid-Atlantic Ridge: Rainbow, Saldanha and Menez Hom Sites. Unpublished PhD Thesis, Dep. Geologia, Universidade de Lisboa, 400 p

Donval JP, Charlou JL, Douville E, Knoery J, Fouquet Y, Ponseveras E, Baptiste PJ, Stievenard M, German C, FLORES scientific party (1997) High H₂ and CH₄ content in hydrothermal fluids from Rainbow site newly sampled at 36°14'N on the AMAR segment, Mid-Atlantic Ridge (diving FLORES cruise, July 1997). Comparison with other MAR sites. *EOS Abst* 78: 832

Dosso L, Bougault H, Langmuir C, Bollinger C, Bonnier O, Etoubleau J (1999) The age and distribution of mantle heterogeneity along the Mid-Atlantic Ridge (31-41°N). *Earth Planet Sci Lett* 170: 269-286

Douville E, Bienvenu P, Charlou JL, Donval JP, Fouquet Y, Appriou P, Gamo T (1999) Yttrium and rare earth elements in fluids from various deep-sea hydrothermal systems. *Geochim Cosmochim Acta* 63: 627-643

Douville E, Charlou JL, Donval JP, Knoery J, Fouquet Y, Bienvenu P, Appriou P, FLORES scientific party (1997) Trace elements in fluids from the new Rainbow hydrothermal field (36°14'N, MAR): a comparison with other Mid-Atlantic Ridge fluids. *EOS Abst* 78: 832

Douville E, Charlou JL, Oelkers EH, Bienvenu P, Jove Colon CF, Donval JP, Fouquet Y, Prieur D, Appriou P (2002) The Rainbow vent fluids (36°14'N, MAR): the influence of ultramafic rocks and phase separation on trace metal content in Mid-Atlantic Ridge hydrothermal fluids. *Chem Geol* 184: 37-48

Doyle M, Allen R (2003) Subsea-floor replacement in volcanic-hosted massive sulfide deposits. *Ore Geol Rev* 23: 183-222

Drummond SE, Ohmoto H (1985) Chemical evolution and mineral deposition in boiling hydrothermal systems. *Econ Geol* 80: 126-147

Edmonds HN, German C (2004) Particle geochemistry in the Rainbow hydrothermal plume, Mid-Atlantic Ridge. *Geochim Cosmochim Acta* 68: 759-772

Farkas A (1980) The distribution of cobalt and nickel between pyrite and pyrrhotite. Unpublished PhD Thesis, Dep. Geology, University of Toronto, 181 p

FLORES Cruise Report (1998) IFREMER, France

Fouquet Y, Stackelberg U, Charlou JL, Erzinger J, Herzig PM, Mühe R and Wiedicke M (1993a) Metallogenesis in back-arc environments: the Lau Basin Example. *Econ Geol* 88: 2154-2181

Fouquet Y, Wafik A, Cambon P, Mevel C, Meyer G, Gente P (1993b) Tectonic setting and mineralogical and geochemical zonation in the Snake Pit sulfide deposit (Mid-Atlantic Ridge at 23 °N). *Econ Geol* 88: 2018-2036

Fouquet Y, Knott R, Cambon P, Fallick A, Rickard D, Desbruyeres D (1996) Formation of large sulfide mineral deposits along fast spreading ridges. Example from off-axial deposits at 12°43'N on the East Pacific Rise. *Earth Planet Sci Lett* 144: 147-162

Früh-Green G, Kelley DS, Bernasconi SM, Karson JA, Ludwig KA, Butterfield DA, Boschi C, Proskurowski G (2003) 30000 years of hydrothermal activity at the Lost City vent field. *Science* 301: 495-498

Fyfe WS (1992) Geosphere interactions on a convecting planet: Mixing and separation. In: Hutzinger O (ed) *The handbook of environmental chemistry* 1. Springer-Verlag, pp 1-26

German C, Higgs NC, Thomson J, Mills RA, Elderfield H, Blusztajn J, Fler AP, Bacon MP (1993) A geochemical study of metalliferous sediment from the TAG hydrothermal mound 26°08'N Mid-Atlantic Ridge. *J Geophys Res* 98: 9683-9692

German C, Klinkhammer CP, Rudnicki MD (1996) The Rainbow hydrothermal plume, 36°15'N, MAR. *Geophys Res Lett* 23(21): 2979-2982

Green AH, Naldrett AJ (1981) The Langmuir volcanic peridotite-associated nickel deposits: Canadian equivalents of the Western Australian occurrences. *Econ Geol* 76: 1503-1523

Goodfellow WD, Franklin JM (1993) Geology, mineralogy, and chemistry of sediment-hosted clastic massive sulfides in shallow cores, Middle Valley, Northern Juan de Fuca Ridge. *Econ Geol* 88: 2037-2068

Gràcia E, Charlou JL, Knoery J, Parson LM (2000) Non-transform offsets along the Mid-Atlantic Ridge south of the Azores (38°N-34°N): ultramafic exposures and hosting of hydrothermal vents. *Earth Planet Sci Lett* 177: 89-109

Hannington MD, Jonasson IR, Herzig PM, Petersen S (1995) Physical and chemical processes of seafloor mineralization at mid-ocean ridges. In: Humphris SE, Zierenberg RA, Mullineaux LS, Thomson RE (eds) *Seafloor hydrothermal systems: physical, chemical, biological and geological interactions (Geophysical Monograph 91)* American Geophysical Union, pp 466

Hawley JE, Nichol I (1961) Trace elements in pyrite, pyrrhotite and chalcopyrite of different ores. *Econ Geol* 56: 467-487

Herzig PM, Hannington MD (1995) Polymetallic massive sulfides at the modern seafloor A review. *Ore Geol Rev* 10: 95-115

Herzig PM, Petersen S, Hannington MD (1998) Geochemistry and sulphur-isotopic composition of the TAG hydrothermal mound, Mid-Atlantic Ridge, 26°N. In: Herzig PM, Humphris SE, Miller DJ, Zierenberg RA (eds) *Proceedings of the Ocean Drilling Program Scientific Results* 158: 47-70

Humphris SE, Herzig PM, Miller S, Alt JC, Becker K, Brown D, Brüggmann G, Chiba H, Fouquet Y, Gemmell JB, Guerin JB, Hannington MD, Holm MD, Honnorez J, Iturrino JJ, Knott GJ, Ludwig R, Nakamura K, Petersen S, Reysenbach A, Rona PA, Smith D, Sturz A, Tivey MK, Zhao X (1995) The internal structure of an active seafloor massive sulphide deposit. *Nature* 377: 713-716

Huston DL, Sie SH, Suter GF (1995) Selenium and its importance to the study of ore genesis: the theoretical basis and its application to volcanic-hosted massive sulfide deposits using pixeprobe analysis. *Nucl Instr Meth Phys Res B* 104: 476-480

Hutchinson MN, Scott SD (1981) Sphalerite geobarometry in the Cu-Fe-Zn-S system. *Econ Geol* 76: 143-153

IRIS Cruise Report (2001) IFREMER, France

James RH, Elderfield H, Palmer MR (1995) The chemistry of hydrothermal fluids from the Broken Spur site, 29°N Mid-Atlantic Ridge. *Geochim Cosmochim Acta* 59: 651-659

Janecky DR, Seyfried Jr. WE (1986) Hydrothermal serpentinization of peridotite within the oceanic crust: Experimental investigations of mineralogy and major element chemistry. *Geochim Cosmochim Acta* 50: 1357-1378

- Kase K, Yamamoto M, Shibata T (1990) Copper-rich sulfide deposit near 23°N, Mid-Atlantic Ridge: chemical composition, mineral chemistry, and sulphur isotopes. In: Detrick R, Honnorez J, Bryan WB, Juteau T (eds) Proceedings of the Ocean Drilling Program Scientific Results, pp 163-175
- Kelley D, Karson JA, Blackman DK, Früh-Green GL, Butterfield D, Lilley MD, Olson E, Schrenk M, Roe K, Lebon GT, Rivizzigo P, AT3-60 scientific party (2001) An off-axis hydrothermal vent field near the Mid-Atlantic Ridge at 30°N. *Nature* 412: 145-149
- Kojima S, Sugaki A (1985) Phase relations in the Cu-Fe-Zn-S System between 500° and 300° under hydrothermal conditions. *Econ Geol* 80: 158-171
- Lacan F (2002) Masses d'eau des mers nordiques et de l'Atlantique subarctique tracées par les isotopes du néodyme Laboratoire des études géophysiques et océanographiques spatiales. Université Toulouse III - Paul Sabatier, Toulouse, pp 293.
- Langmuir C, Humphris SE, Fornari DJ, Van Dover C, Von Damm KL, Tivey MK, Colodner D, Charlou JL, Desonie D, Wilson C, Fouquet Y, Klinkhammer G, Bougault H (1997) Hydrothermal vents near a mantle hot spot: the Lucky Strike vent field at 37°N on the Mid-Atlantic Ridge. *Earth Planet Sci Lett* 148: 69-91
- Large R (1992) Australian volcanic-hosted massive sulfide deposits: features, styles, and genetic models. *Econ Geol* 87: 471-510
- Lawrie D, Miller DJ (2000) Data Report: Sulfide mineral chemistry and petrography from Bent Hill, ODP Mound and TAG massive sulfide deposits. In: Zierenberg RA, Fouquet Y, Miller DJ, Normak WR (eds) Proceedings Ocean Drilling Program Scientific Results, pp 1-34
- Lein AY, Ulyanova NV, Ulyanov A, Cherkashev δ , Stepanova T (2001) Mineralogy and geochemistry of sulfide ores in ocean-floor hydrothermal fields associated with serpentine protrusions. *Russ J Earth Sci* 3(5)
- Loftus-Hills G, Solomon M (1967) Cobalt, nickel and selenium in sulphides as indicators of ore genesis. *Miner Deposita* 2: 228-242

- Loukola-Ruskeeniemi K (1999) Origin of black shales at the serpentinite-associated Cu-Zn-Co ores at Outokumpu, Finland. *Econ Geol* 94: 1007-1028
- Lowell RP, Rona PA (2002) Seafloor hydrothermal systems driven by the serpentinization of peridotite. *Geophys Res Lett* 29: 26-1, 26-4
- Marques AFA, Barriga FJAS, Fouquet Y (2003) Co:Ni ratio variation throughout the Rainbow Hydrothermal System. In: Eliopoulos DG et al. (eds) Mineral exploration and sustainable development. Proceedings of the Seventh Biennial SGA Meeting, Athens, Greece, 24-28 August 2003. Millpress, Rotterdam, pp 143-146
- MacDonald AM, Fyfe WS (1985) Rate of serpentinization in seafloor environments. *Tectonophysics* 116: 123-135
- McDonough WF, Sun S (1995) The composition of the Earth. *Chem Geol* 120: 223-253
- Mével C (2003) Serpentinization of abyssal peridotites at mid-ocean ridges. *C. R. Geoscience* 335: 825-852
- Michard A, Albarède F (1986) The REE content of some hydrothermal fluids. *Chem Geol* 55: 51-60
- Mills RA, Elderfield H (1995) Rare earth element geochemistry of hydrothermal deposits from the active TAG mound, 26° north, Mid-Atlantic Ridge. *Geochim Cosmochim Acta* 59: 3511-3524
- Moody JB (1976) Serpentinization: a review. *Lithos* 9: 125-138
- Mookherjee A, Philip R (1979) Distribution of copper, cobalt and nickel in ores and host rocks, Ingladhol, Karhataka, India. *Miner Deposita* 14: 33-55
- Münch U, Blum N, Halbach P (1999) Mineralogical and geochemical features of sulfides from the MESO zone, Central Indian Ridge. *Chem Geol* 155: 29-44
- Niu Y, Bideau D, Hekinian R, Batiza R (2001) Mantle compositional control on the extent of mantle melting crust production, gravity anomaly, ridge morphology, and ridge segmentation: a case study at the Mid-Atlantic Ridge 33-35°N. *Earth Planet Sci Lett* 186: 383-399
- O'Hanley DS (1992) Solution to the volume problem in serpentinization. *Geology* 20: 705-708

O'Hanley DS (1996) *Serpentinities. Records of Tectonics and Petrological History*. Oxford University Press, New York, 277p

Palandri JL, Reed MH (2004) Geochemical models of metasomatism in ultramafic systems: serpentinization, rodingitization, and sea floor carbonate chimney precipitation. *Geochim Cosmochim Acta* 68: 1115-1133

Parson L, Fouquet Y, Ondréas H, Barriga FJAS, Relvas JMR, Ribeiro A, Charlou JL, German C, FLORES scientific party (1997) Non-Transform discontinuity settings for contrasting hydrothermal systems on the MAR-Rainbow and FAMOUS at 36°14' and 36°34'N. *EOS Abst* 78: 832

Peter J, Scott SD (1997) Windy Craggy, northwestern British Columbia: the world's largest Besshi-type deposit In: Barrie CT, Hannington MD (eds) *Volcanic associated massive sulfide deposits: processes and examples in modern and ancient settings*, Society of Economic Geologists. 8, pp 295-329

Rona PA, Hannington MD, Raman CV, Thompson G, Tivey MK, Humphris SE, Lalou C, Petersen S (1993) Active and relic sea-floor hydrothermal mineralization at the TAG hydrothermal field, Mid-Atlantic Ridge. *Econ Geol* 88: 1989-2017

Saldanha Cruise Report (1999) Universidade de Lisboa, Portugal

Saunders AD, Norry MJ, Tarney J (1988) Origin of MORB and chemically depleted mantle. *J Petrol (Special Lithosphere Issue)*: 415-445

Seewald JS, Seyfried Jr WE (1990) The effect of temperature on metal mobility in sub seafloor hydrothermal systems: constraints from basalt alteration experiments. *Earth Planet Sci Lett* 101: 388-403

Seahma Cruise Report (2003) Universidade de Lisboa, Portugal

Seyfried Jr WE, Dibble Jr WE (1980) Seawater-peridotite interaction at 300° C and 500 bars: implications for the origin of oceanic serpentinites. *Geochim Cosmochim Acta* 44: 309-321

Seyfried Jr WE, Berndt ME, Janecky D (1986) Chloride depletions and enrichments in seafloor hydrothermal fluids: constraints from experimental basalt alteration studies. *Geochim Cosmochim Acta* 50: 469-475

Seyfried Jr WE, Ding K (1995) Phase equilibria in sub seafloor hydrothermal systems: a review of the role of redox, temperature, pH and dissolved Cl on the chemistry of hot spring fluids at mid-ocean ridges. In: Humphris SE, Zierenberg

RA, Mullineaux LS, Thomson RE (eds) Seafloor hydrothermal systems: Physical, chemical, biological and geological interactions (Geophysical Monograph 91) American Geophysical Union 91: 248-272

Schilling JG, Zajac M, Evans R, Johnston T, White WM, Devine JD and Kingsley R (1983) Petrological and geochemical variations along the Mid-Atlantic Ridge from 29°N-73°N. *Am J Sci* 283: 510-586

Schroeder T, John B, Frost B (2002) Geologic, implications of seawater circulation through peridotite exposed at slow-spreading mid-ocean ridges. *Geology* 30: 367-370

Thurnherr AM, Richards KJ (2001) Hydrography and high-temperature heat flux of the Rainbow hydrothermal site (36°14'N, Mid-Atlantic Ridge). *J Geophys Res* 106: 9411-9426

Thurnherr AM, Richards KJ, German CR, Lane-Serff GF, Speer KG (2002) Flow and mixing in the rift valley of the Mid-Atlantic Ridge. *J Phys Ocean* 132: 1763-1778

Tivey MK, Humphris SE, Thompson G, Hannington MD, Rona PA (1995) Deducing patterns of fluid flow and mixing within the active TAG hydrothermal mound using mineralogical and geochemical data. *J Geophys Res* 100: 12527-12555

Vaughan DJ, Craig JR (1997) Sulfide ore stabilities, morphologies and intergrowth textures. In: Barnes HL (ed) *Geochemistry of hydrothermal ore deposits* (3rd edn). Wiley, New York, pp 367-434

Von Damm KL (1995) Controls on the chemistry and temporal variability of seafloor hydrothermal fluids. In: Humphris SE, Zierenberg RA, Mullineaux LS, Thomson RE (eds) *Seafloor hydrothermal systems: physical, chemical, biological and geological interactions* (Geophysical Monograph 91) American Geophysical Union pp 222-247

Walshe JL, Solomon M (1981) An investigation into the environment of formation of the volcanic-hosted Mt. Lyell copper deposits using geology, mineralogy, stable isotopes and a six component chlorite solid solution model. *Econ Geol* 76: 246-280

Wetzel L, Shock EL (2000) Distinguishing ultramafic from basalt hosted submarine hydrothermal systems by comparing calculated vent fluid compositions. *J Geophys Res* 105: 8319-8340